

Onboard Model-based Prediction of Tram Braking Distance^{*}

Loi Do^{*} Ivo Herman^{**} Zdeněk Hurák^{***}

^{*} Faculty of Electrical Engineering, Czech Technical University in Prague, CZ (e-mail: doloi@fel.cvut.cz).

^{**} Herman Elektronika, Brno, CZ (e-mail: ivo.herman@herman.cz).

^{***} Faculty of Electrical Engineering, Czech Technical University in Prague, CZ (e-mail: hurak@fel.cvut.cz)

Abstract: In this paper, we document design and a prototype implementation of a computational method for an onboard prediction of a braking distance for a city rail vehicle—a tram. The method is based on an onboard simulation of tram braking dynamics. Inputs to this simulation are the data from a digital map and the estimated (current) position and speed, which are, in turn, estimated by combining a mathematical model of dynamics of a tram with the measurements from a GNSS/GPS receiver, an accelerometer and the data from a digital map. Experiments with real trams verify the functionality, but reliable identification of the key physical parameters turns out critically important. The proposed method provides the core functionality for a collision avoidance system based on vehicle-to-vehicle (V2V) communication.

Keywords: Automatic control, optimization, real-time operations in transportation, Simulation, Braking distance prediction, Rail transport, Mathematical modeling

1. INTRODUCTION

1.1 Motivation, short description

In this paper, we present a computational method for prediction of a tram braking distance based on an onboard simulation of a mathematical model of tram braking dynamics. The proposed algorithm runs onboard the tram. It combines in real time the outputs from the mathematical model of longitudinal dynamics of the tram with the signals provided by a GNSS/GPS receiver, an inertial measurement unit (IMU), and the data read from a digital map.

The motivation for such development is the disturbingly high number of collisions of trams with other trams, other vehicles, and even pedestrians¹. Different collision scenarios call for different approaches to their solutions. In the research described in this paper, we restrict ourselves to collisions between vehicles. In particular, we consider tram-to-tram collisions. The reason for considering collisions between trams is that both participants in the (potential) collision are operated by a single organization/company, which makes coordinated collision avoidance schemes (almost) immediately realizable. The key technology for such coordination is wireless vehicle-to-vehicle (V2V) communication, through which the trams could exchange their position and speed estimates and predictions, thus truly distributed estimation/predictions could be realized.

The parameters of the model of dynamics of the tram can be partially determined from the technical specifications provided by the producer and partially extracted from data measured using onboard sensors during experiments (grey box identification). Although in this paper, we consider one particular tram brand and type, the proposed procedure can be applied to any (light) rail vehicle.

1.2 State of the art

In general, real time prediction of braking distance (or motion in general) of rail vehicles plays an important role in *safety* application (Lehner et al., 2009), (Gu et al., 2013), (Wu et al., 2018) or *energy optimization* (Lu et al., 2016), (Keskin and Karamancioglu, 2016). For safety applications involving suburban or freight trains, the prediction of braking distance need not be accurate due to relatively large gap distance (to the next train) and approximately constant parameters of the train dynamics. Simple braking distance prediction models based only on constant parameters of heavy-weight trains their current speed and track characteristics have been published (IEEE, 2009). In cities with a dense tram network, however, the distance gap between two (rail or road) vehicles could go down to a few meters (stopping at tram stops or traffic lights), resulting in a higher probability of collisions. This imposes higher requirements on the accuracy of related onboard estimations and predictions which are, in turn, conditioned by the accurately identified physical parameters. The parameters are mainly the weight of the vehicle, which is given by the actual number of passengers (the total weight of the tram can be some 50 % higher from an empty tram), the coefficients characterizing the adhesion conditions (given by humidity, temperature), slope of the track (tramways).

^{*} The research was funded by Technology Agency of the Czech Republic within the program Epsilon, the project TH03010155.

¹ Prague Public Transit, Co. Inc. has been registering well above one thousand collisions every year.

Not many works in the literature seem to be systematically addressing these issues.

One component of the full collision avoidance system is an estimator of the (distance) gap, that is, the distance between the rear bumper of the leading vehicle and the front bumper of the following vehicle. One class of these estimators is based on vision-based techniques (Mukhtar et al., 2015). An alternative followed in the broader project, within which we write this paper, is to use the V2V communication (Xiang et al., 2014), (Abboud et al., 2016) between the two vehicles and, effectively, realize an estimator of the distance gap in a distributed manner. Nonetheless, in this paper, we do not elaborate further on this topic of the distance gap estimation.

1.3 Outline of the paper

This paper is structured as follows. In Sec. 2, we give some background information about the Tatra T3 tram. We also describe the instrumentation used for onboard measurements. Then in Sec. 3 we describe the model of dynamics with the values of the physical parameters identified from real data obtained in experiments with trams and document the verification of the model. In Sec. 4, we describe the use of the model for prediction of braking distance and describe in more detail estimation of the position and the speed of a tram. We also compare the proposed method with a simple equation-based braking distance prediction method. Lastly, we give a conclusion in Sec. 5.

2. EXPERIMENTAL SETUP

2.1 Tatra T3 tram

We focus on developing a model of dynamics of the Tatra T3 tram partially parametrized by data acquired onboard a tram during experiments. With nearly 14 thousand produced trams during the period from 1960 to 1989, the T3 tram is one of the most produced tram cars in the world (Mara, 2001). In the Czech Republic, T3 trams (in several modernized versions) are still used nowadays and form a significant portion of public transport tram fleets in many cities. Proportions of the tram and parameters relevant for the modeling are listed in Tab. 1 (Linert et al., 2005).

2.2 Instrumentation

The instrumentation in the T3 tram measures only a few values, for instance, tram speed (computed from a wheel

Table 1. Parameters of the T3 tram.

Parameter	Notation	Value
Curb weight	-	$\approx 16\,500$ kg
Gross weight	-	$\approx 27\,500$ kg
Body length	-	14 000 mm
Body height	-	3060 mm
Body width	-	1440 mm
Wheel radius	r	325 mm
Wheel mass	m_w	195 kg
Total motors power	P_{\max}	4×44 kW
Maximum speed	-	65 km h $^{-1}$

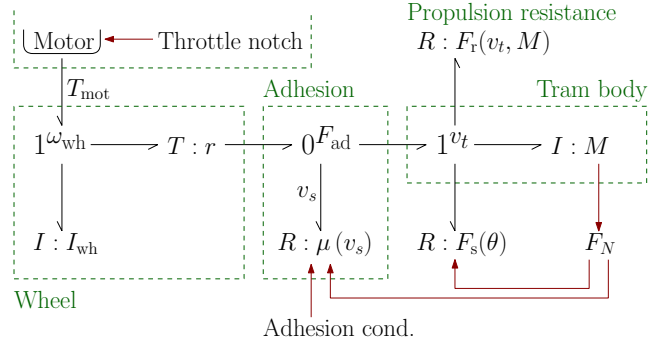


Fig. 1. Bond graph of longitudinal motion dynamics.

speed) or applied current to motor. Also, we could not directly read the data during the experiments (lack of the CAN bus). We, therefore, used external instrumentation to collect the measurements for the model identification. We used GNSS receiver *NEOM8P* by *U-blox* to measure the position and the speed of the tram and inertial measurement unit (IMU) *ADIS16465-1BMLZ* by *Analog devices* to measure the acceleration. We used ready-to-use application/evaluation boards from the manufacturer to directly read the measurements from the sensors. We set the sampling frequency of the GNSS/GPS receiver to 1 Hz and the sampling frequency of the IMU to 2 kHz. We aligned the x-axis of IMU with the direction of the longitudinal motion of the tram.

3. MODEL OF DYNAMICS

3.1 Identification of a model

For the prediction of braking distance, it is sufficient to use the quarter model of dynamics describing only the longitudinal motion of a tram (Sadr et al., 2016). The quarter model of dynamics is given by equations:

$$J_{\text{wh}}\dot{\omega}_{\text{wh}} = (T_{\text{mot}} - rF_{\text{ad}}), \quad (1a)$$

$$M\dot{v}_t = (F_{\text{ad}} - F_r - F_s), \quad (1b)$$

where ω_{wh} is angular speed of the wheel, J_{wh} is moment of inertia of the wheel, T_{mot} is torque given from the motors, r is radius of a wheel, F_{ad} is adhesion force, v_t is longitudinal speed of the tram, M is total weight of the tram, F_r and F_s are resistive forces. This model can be also described by a *bond graph* (Brown, 2006) displayed in Fig. 1. Approximating the wheel as a homogeneous disk, we can write its moment of inertia as:

$$J_{\text{wh}} = 0.5m_w r^2. \quad (2)$$

The total weight of the tram M is sum of the curb weight and weight of passengers in the tram. The torque T_{mot} generated by the motors is proportional to the notch (position) of the control throttle. In the T3, the throttle control has in total 15 notches: seven notches for acceleration, seven notches for deceleration, and one notch for idle. We identified the traction characteristics experimentally as:

$$\tilde{T}_{\text{mot}}(p) = \begin{cases} 1449p & \text{for } p \geq 0 \text{ and } \tilde{T}_{\text{mot}}\omega_{\text{wh}} < P_{\max}, \\ P_{\max}/\omega_{\text{wh}} & \text{for } p \geq 0 \text{ and } \tilde{T}_{\text{mot}}\omega_{\text{wh}} \geq P_{\max}, \\ 1176p & \text{for } p < 0, \end{cases} \quad (3)$$

where $p \in \{-7, -6, \dots, 0, \dots, 6, 7\}$ is the notch. The constants (1449 and 1176) were set to match experimentally

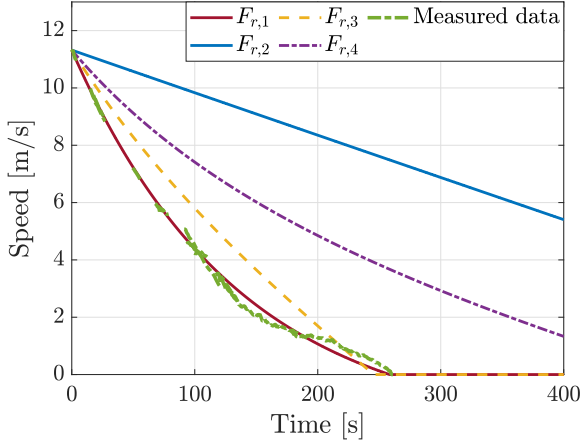


Fig. 2. Comparison of identified parameters for propulsion resistance and parameters from literature.

measured maximal and minimal acceleration at the highest and lowest notch, respectively. Braking torque is not restricted by the P_{\max} . Also, we model the dynamics of the change of \tilde{T}_{mot} as first order system:

$$T_{\text{mot}}(t) = 3e^{-3t}\tilde{T}_{\text{mot}}(p). \quad (4)$$

The adhesion force F_{ad} accounts for the transfer of wheel speed into the longitudinal motion of the tram body. A physical explanation of the adhesion is given in Park et al. (2008). In general, the adhesion force F_{ad} is computed as a sum of adhesion force given by each traction wheel and the adhesion force is proportional to the wheel load. However, since all wheels of T3 tram are connected to the traction motors and by assuming the uniform distribution of the tram weight on each wheel, we can directly write:

$$F_{\text{ad}} = \mu(v_s)F_N, \quad (5a)$$

$$F_N = Mg, \quad (5b)$$

$$v_s = r\omega_{\text{wh}} - v_t, \quad (5c)$$

$$\mu(v_s) = c_a e^{-a_a v_s} - d_a e^{-b_a v_s}, \quad (5d)$$

where g is gravitational acceleration. Parameters a_a , b_a , c_a and d_a vary on track conditions (Takaoka and Kawamura, 2000).

Propulsion resistance F_r of rail vehicles (sum of rolling and air resistance) is typically calculated using an empirical equation in a form (Hay, 1982):

$$F_r(v_t) = A + Bv_t + Cv_t^2, \quad (6)$$

where A , B and C are coefficients giving the dependence of propulsion resistance on characteristics of the rail vehicle such as weight, number of axles or front surface cross-sectional area. To identify coefficients in Eq. (6) we first gather all measurements from experiments during which the tram decelerate only due to propulsion resistance (idle notch), see Fig. 2 (*Measured data*). Note, that we could not obtain longer continuous decay from higher speeds due to the restriction of the test track. We can simulate the model and set the same conditions as in the experiments to find appropriate coefficients. The weight of the tram during experiments was 17 000 kg (estimated from a number of people in the tram during the experiment). Since trams usually operate at lower speeds than other trains, we simplify the identification of Eq. (6) by neglecting quadratic

dependence on v_t , thus setting $C = 0$. The identified propulsion resistance equation is:

$$F_{r,1}(v_t, M) = 0.0147M + 125.83v_t. \quad (7)$$

The reason why we do not use coefficients of Eq. (6) from the literature is that they are usually designed for rail vehicles which have significantly higher weight and also operate at higher speeds than trams. For instance, using the following equations from the literature evaluated for the T3 tram yields:

$$F_{r,2}(v_t, M) = 0.0147M + 2.18 \times 10^{-6}Mv_t^2, \quad (8a)$$

$$F_{r,3}(v_t, M) = 520 + 0.0065M + 3.6v_t + 3.8880v_t^2, \quad (8b)$$

$$F_{r,4}(v_t, M) = 1.839\sqrt{M} + 0.0036Mv_t + 4.329v_t^2. \quad (8c)$$

Propulsion resistance $F_{r,2}$ was designed for passenger train on bogies (Iwnicki, 2006), $F_{r,3}$ for electric locomotive and $F_{r,4}$ for suburban electric multiple unit train (Rochard and Schmid, 2000). See the comparison in Fig. 2. We can see that the speed decay when using any of Eq. (8) does not match with the measurements.

Lastly, in addition to propulsion resistance, the motion of a tram is also affected by the slope θ (longitudinal inclination) of track:

$$F_s(\theta) = F_N \sin \theta. \quad (9)$$

Slope θ is positive for ascent and negative for the descent.

3.2 Verification of a model

To verify the model with experimentally obtained data, we first remove the noise and bias in the measured data from the accelerometer. The noise was contained in the measurements mainly due to vibrations onboard of a tram and sensor noise. Since the longitudinal dynamics of a tram is relatively slow, we used the low-pass filter with the cut-off frequency 2 Hz. We verify the model by setting the same sequence of the throttle notches, as in real experiments for two scenarios. In the scenario in Fig. 3, the driver was instructed to set the maximal acceleration for a certain amount of time and then set the maximal deceleration. We can see, that around time 5 s, $T_{\text{mot}}\omega_{\text{wh}} \geq P_{\max}$ which results in decline of T_{mot} . The total actual and simulated traveled distance during the experiment is 217 m and 207 m, respectively. The scenario in Fig. 4 has a more complicated sequence of throttle notches. The total actual and simulated traveled distance during this scenario is 158 m and 164 m, respectively. We can see that the modeled dynamics of the acceleration and the speed is similar to the experimental data. Note that the discrepancies in total simulated and actual traveled distances are caused by a small error in generated acceleration, which is integrated twice.

The tram body at the moment of the stop exhibits oscillation due to the mechanics in the bogies. This effect is not incorporated into the model since it does not affect the braking distance.

We will conduct another verification experiments with varying conditions (different track, adhesion conditions, and a total weight M of the tram) by the end of the year 2019.

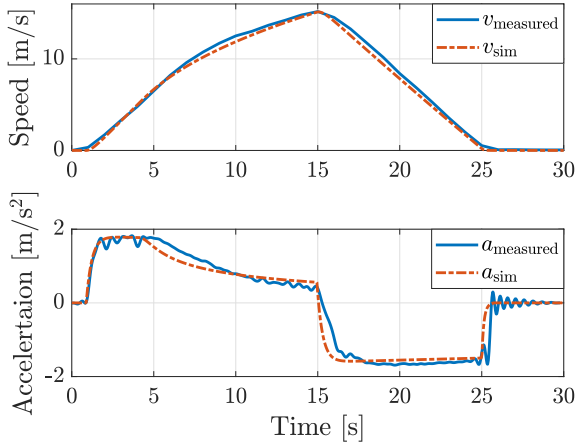


Fig. 3. Comparison of the model and real measurements for given sequence of throttle notches: maximal and minimal acceleration.

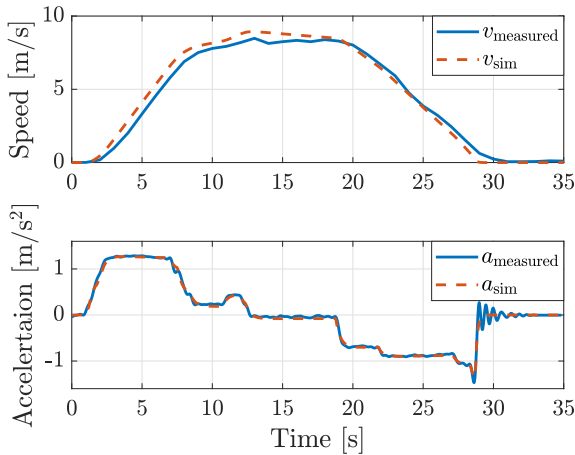


Fig. 4. Comparison of the model and real measurements for given sequence of throttle notches.

4. BRAKING DISTANCE PREDICTION

To predict the braking distance using the model of dynamics, we first measure (or estimate) the speed v_t of the tram. The speed v_t can be estimated, for instance, by fusing measurements from GNSS, IMU (Bar-Shalom et al., 2008), and possibly the wheel speed (Ararat and Söylemez, 2017). The value of the speed v_t is then used as an initial condition in the simulation of the model. We can then simulate the model with a selected notch ($p \leq 0$) and obtain the braking distance as the total traveled longitudinal distance from the start of the simulation until the tram reaches the speed $v_t = 0$. Since the simulation of the proposed model is not computationally intensive, the simulation can be run periodically in real time onboard a tram, for instance, synchronously with the estimation of the speed v_t .

To get correct results, we need also to estimate all following time varying parameters:

- Adhesion conditions: Estimation of the adhesion conditions (coefficients of $\mu(v_s)$) is well covered by vari-

ous methods (Sadr et al., 2016), (Pichlik and Zdenek, 2018).

- Slope: The slope θ of the track can be retrieved from known absolute position and the digital map.
- Weight: The weight M could be estimated, for instance, from number of passengers in the tram counted by sensors at the tram entrances.

In the work which we present in this paper, we extensively focused only on estimation of the position and the speed. We assume that the total weight and the adhesion conditions are known.

4.1 Position and speed estimation

To estimate the position and the speed of a tram, we use discrete Kalman Filter with measurements from IMU, GNSS/GPS receiver, and the digital map. We first need to rewrite the equations (1) and (5) into the discrete state-space representation. Also, since we can not measure the motion of the wheel, nor the input from the driver in the T3 tram, we simplify the equations by assuming constant longitudinal acceleration:

$$\begin{bmatrix} x_{k+1} \\ v_{k+1} \\ a_{k+1} \end{bmatrix} = \begin{bmatrix} 1 & \Delta t & 0.5\Delta t^2 \\ 0 & 1 & \Delta t \\ 0 & 0 & 1 \end{bmatrix} \begin{bmatrix} x_k \\ v_k \\ a_k \end{bmatrix}, \quad (10)$$

where Δt is sample time, x_k , v_k , and a_k are respectively the longitudinal traveled distance, the speed, and the acceleration. The change in the acceleration a_k is realized (when using the Kalman Filter) through the measurements. The output equation is:

$$y_k = \begin{bmatrix} x_k \\ v_k \\ a_k \end{bmatrix}. \quad (11)$$

One problem with this description is that the GNSS receiver measures position as an absolute geographic coordinate y_{GPS} , whereas the model output is longitudinal distance. We resolve this problem by creating a mapping from y_{GPS} into longitudinal distance x by use of a digital map of the track so the real measurement can be compared with model output. The principle of the mapping is as follows: we first project the measured absolute geographic position y_{GPS} onto the track. Then, we can compute traveled longitudinal distance x from some selected reference point on the track $x = 0$ (such as a depot or first tram stop) to the projected point. See Fig. 5 for an illustration. The estimated absolute position, in combination with a digital map, also gives the current slope θ .

4.2 Comparison of braking distance prediction methods

We now compare the proposed method for braking distance (model-based) prediction with the prediction using an equation (equation-based) derived from simple kinematics:

$$d_{\text{br}} = 0.5v_t^2 a_{\text{dec}}^{-1}, \quad (12)$$

where d_{br} is calculated braking distance and a_{dec} is selected braking deceleration. Such calculation of braking distance for rail vehicles has been published (IEEE, 2009) and used in several works (Lu et al., 2016), (Wu et al., 2018) due to its simplicity.

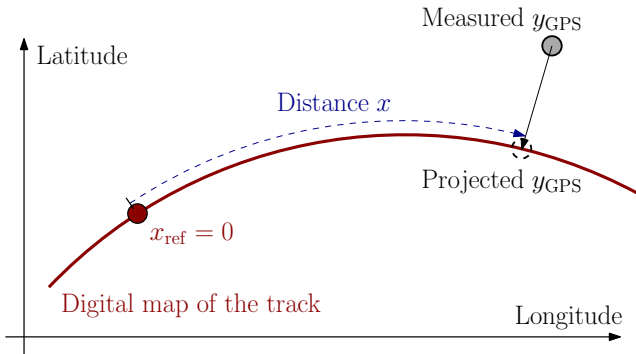


Fig. 5. Illustration of projection of measured point y_{GPS} .

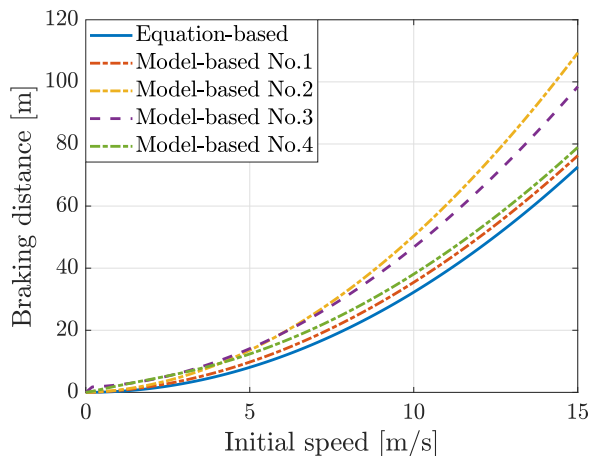


Fig. 6. Comparison of equation-based and model-based prediction of braking distance.

To get comparable results from equation-based and model-based methods, we set maximal deceleration of equation-based prediction (12) to $a_{dec} = 1.55 \text{ m s}^{-2}$ which approximately corresponds to maximal measured deceleration of empty tram with zero slope and dry adhesion conditions. We set such physical parameters in the simulation, see Fig. 6, simulation No. 1. We can see that the equation-based model gives in general lower braking distance (at 15 m s^{-1} lower by $\approx 4 \text{ m}$). The difference is mainly to the fact that model-based calculation, unlike the equation-based calculation, takes into account also the limited dynamics of deceleration.

For illustration, we also simulate the model with various parameters, see Tab. 2. Adhesion coefficients $[a_a, b_a, c_a, d_a]$ for dry conditions are: $[0.54, 1.2, 1, 1]$ and for wet conditions: $[0.05, 0.5, 0.08, 0.08]$ (Takaoka and Kawamura, 2000). From the simulation No. 2, we can observe, that even though a higher weight cause higher propulsion resistance, it also decrease maximal braking effort which results in significantly higher braking distance. Braking distance is also significantly affected by the relatively small (negative) slope, as we can see from simulation No. 3. Simulation No. 4 shows that worse adhesion conditions have a relatively higher effect on the braking distance at lower speeds ($\approx 5 \text{ m s}^{-1}$).

Table 2. Parameters of the simulations.

Sim. No.	Notch p	M [kg]	Slope θ [rad]	Adh. cond.
1	-7	17 000	0	Dry
2	-7	25 000	0	Dry
3	-7	17 000	-0.035	Dry
4	-7	17 000	0	Wet

5. CONCLUSION AND FUTURE RESEARCH

In this paper, we presented a method for prediction of tram braking distance based on real time simulation of a model of dynamics of a tram. The braking distance prediction algorithm runs onboard a tram, taking as the inputs estimated longitudinal speed of a tram and key time-varying physical parameters affecting the braking distance such as the total weight of the tram, adhesion conditions, or the slope of the track. We have shown, through various simulations, that predicted braking distance significantly depends on values of the physical parameters. For safety applications such as collision avoidance, which is the ultimate goal of this research, the accurate prediction of braking distance is crucial for the correct detection of imminent collisions.

Besides the safety applications, within which we have written this paper, the model can be used in other applications such as energy optimization or slip control. As a model of dynamics, we used a quarter model for a rail vehicle. We identified the parameters of the model partially from the literature and partially from the data measured using onboard sensors during real experiments. Also, by comparing the simulations of the model with real experiments, we verified its correctness. Another verification experiments with different physical parameters will be done by the end of the year 2019. The implemented model in Matlab and Simulink is downloadable at <https://www.mathworks.com/matlabcentral/fileexchange/73391>.

ACKNOWLEDGEMENTS

Significant help from Vt Obrusnk with conducting the experiments is acknowledged. We would also like to express our gratitude to the engineers from Ostrava Public Transit Co. Inc. (Dopravn podnik Ostrava, a.s.) for enabling the experiments with trams.

REFERENCES

- Aboud, K., Omar, H.A., and Zhuang, W. (2016). Interworking of DSRC and Cellular Network Technologies for V2x Communications: A Survey. *IEEE Transactions on Vehicular Technology*, 65(12), 9457–9470. doi:10.1109/TVT.2016.2591558. 00006.
- Ararat, Ö. and Söylemez, M.T. (2017). Robust Velocity Estimation for Railway Vehicles. *IFAC-PapersOnLine*, 50(1), 5961–5966. doi:10.1016/j.ifacol.2017.08.1256.
- Bar-Shalom, Y., Li, X.R., and Kirubarajan, T. (2008). *Estimation with Applications to Tracking and Navigation: Theory Algorithms and Software*. Wiley-Interscience, 1st edition.
- Brown, F.T. (2006). *Engineering System Dynamics : A Unified Graph-Centered Approach, Second Edition*. CRC Press. doi:10.1201/b18080.
- Gu, Q., Zuo, H., Su, R., Zhang, K., and Xu, H. (2013). A Wireless Subway Collision Avoidance Sys-

- tem Based on Zigbee Networks. *Journal of Communications*, 8(9), 561–565. doi:10.12720/jcm.8.9.561-565. URL <http://www.jocm.us/index.php?m=content&c=index&a=show&catid=121&id=574>. 00000.
- Hay, W.W. (1982). *Railroad Engineering*. Wiley, New York, 2nd edition.
- IEEE (2009). IEEE Guide for the Calculation of Braking Distances for Rail Transit Vehicles. *IEEE Std 1698-2009*, C1–31. doi:10.1109/IEEESTD.2009.5332051.
- Iwnicki, S. (2006). *Handbook of Railway Vehicle Dynamics*. CRC Press. doi:10.1201/9781420004892. URL <https://www.taylorfrancis.com/books/9781420004892>.
- Keskin, K. and Karamancioglu, A. (2016). Energy Efficient Motion Control for a Light Rail Vehicle Using The Big Bang Big Crunch Algorithm. *IFAC-PapersOnLine*, 49(3), 442–446. doi:10.1016/j.ifacol.2016.07.824.
- Lehner, A., De Ponte Mller, F., Strang, T., and Rico Garca, C. (2009). Reliable vehicle-autarkic collision detection for railbound transportation. In *Proceedings of ITS 2009*. Stockholm, Schweden. URL <http://elib.dlr.de/60056/>. 00008.
- Linert, S., Fojtk, P., and Mahel, I. (2005). *Kolejov vozidla prask mstsk hromadn dopravy*. Praha: Dopravn podnik hl. m. Prahy.
- Lu, S., Wang, M.Q., Weston, P., Chen, S., and Yang, J. (2016). Partial Train Speed Trajectory Optimization Using Mixed-Integer Linear Programming. *IEEE Transactions on Intelligent Transportation Systems*, 17(10), 2911–2920. doi:10.1109/TITS.2016.2535399.
- Mara, R. (2001). *Tatra T3 1960-2000 : 40 let tramvaj Tatra T3*. K-Report.
- Mukhtar, A., Xia, L., and Tang, T.B. (2015). Vehicle Detection Techniques for Collision Avoidance Systems: A Review - IEEE Journals & Magazine. doi:10.1109/TITS.2015.2409109.
- Park, S.H., Kim, J.S., Choi, J.J., and Yamazaki, H.o. (2008). Modeling and control of adhesion force in railway rolling stocks. *IEEE Control Systems Magazine*, 28(5), 44–58. doi:10.1109/MCS.2008.927334.
- Pichlik, P. and Zdenek, J. (2018). Locomotive Wheel Slip Control Method Based on an Unscented Kalman Filter. *IEEE Transactions on Vehicular Technology*, 67(7), 5730–5739. doi:10.1109/TVT.2018.2808379.
- Rochard, B.P. and Schmid, F. (2000). A review of methods to measure and calculate train resistances. *Proceedings of the Institution of Mechanical Engineers, Part F: Journal of Rail and Rapid Transit*, 214(4), 185–199. doi:10.1243/0954409001531306.
- Sadr, S., Khaburi, D.A., and Rodrguez, J. (2016). Predictive Slip Control for Electrical Trains. *IEEE Transactions on Industrial Electronics*, 63(6), 3446–3457. doi:10.1109/TIE.2016.2543180.
- Takaoka, Y. and Kawamura, A. (2000). Disturbance observer based adhesion control for Shinkansen. In *6th International Workshop on Advanced Motion Control. Proceedings (Cat. No.00TH8494)*, 169–174. doi:10.1109/AMC.2000.862851.
- Wu, Y., Wei, Z., Weng, J., and Deng, R.H. (2018). Position Manipulation Attacks to Balise-Based Train Automatic Stop Control. *IEEE Transactions on Vehicular Technology*, 67(6), 5287–5301. doi:10.1109/TVT.2018.2802444.
- Xiang, X., Qin, W., and Xiang, B. (2014). Research on a DSRC-Based Rear-End Collision Warning Model. *IEEE Transactions on Intelligent Transportation Systems*, 15(3), 1054–1065. doi:10.1109/TITS.2013.2293771.